Theor Chem Acc (1998) 99:210–214
DOI 10.1007/s0021498000m7

Theoretical
Chemistry Accounts

Regular article

A theoretical study of the photochemical reductive elimination and thermal oxidative addition of molecular hydrogen from and to the Ir-complex

Y. Hayashi[1], **H. Nakai**[2], **Y. Tokita**[1,4,5], **H. Nakatsuji**[1,3,4]

[1] Department of Synthetic Chemistry and Biological Chemistry, Graduate School of Engineering, Kyoto University, Sakyo-ku, Kyoto 606-01, Japan
[2] Department of Chemistry, School of Science, Waseda University, Shinjuku-ku, Tokyo 169, Japan
[3] Department of Applied Chemistry, Graduate School of Engineering, The University of Tokyo, Hongo, Tokyo 113, Japan
[4] Institute for Fundamental Chemistry, 34-4 Takano Nishihiraki-cho, Sakyo-ku, Kyoto 606-01, Japan
[5] Research Center, Denki Kagaku Kogyo Co. Ltd., 3-5-1 Asahimachi, Machida-shi, Tokyo 194, Japan

Received: 10 December 1997 / Accepted: 16 January 1998 / Published online: 17 June 1998

Abstract. The electronic mechanisms of the cyclic processes of photochemical reductive elimination of H_2 from $[IrClH_2(PH_3)_3]$ and thermal oxidative addition of H_2 to $[IrCl(PH_3)_3]$ are investigated theoretically. The geometries of the ground and excited states are optimized using the Hartree-Fock and single excitation configuration interaction methods, respectively, and higher level calculations for the ground and excited states are carried out by the symmetry adapted cluster (SAC)/SAC–configuration interaction method. The present calculation shows that the reductive elimination of H_2 from $[IrClH_2(PH_3)_3]$ dose not occur thermally but photochemically through diabatic conversion from the lowest A′ excited state to the ground state (A′), while the oxidative addition of H_2 to $[IrCl(PH_3)_3]$ easily proceeds thermally. The lowest $^1A'$ excited state involves the nature of the Ir-H_2 antibonding.

Key words: Iridium complexes – Photochemical reductive elimination of H_2 – Thermal oxidative addition of H_2 – Symmetry adapted cluster (SAC)/SAC-configuration interaction method – Excited states

1 Introduction

The catalytic importance of the iridium complex is one of the most attractive areas of research in organometallic chemistry [1]. While some of these complexes have been shown to undergo oxidative addition of various small molecules [2–14], only a few investigations have examined the photochemical reactivity of the adduct complexes.

Correspondence to: H. Nakatsuji

$[IrClH_2(PPh_3)_3]$ was first prepared by Vaska [15] and has the configuration given in Fig. 1 [16].

This complex does not loose H_2 in the thermal process. In 1976, Geoffroy and Pierantozzi [17] reported that the irradiation of $[IrClH_2(PPh_3)_3]$ with ultraviolet light or sun light results in reductive elimination of H_2 according to the equation

$$\left[IrClH_2(PPh_3)_3\right] \xrightarrow{h\nu} H_2 + \left[IrCl(PPh_3)_3\right]. \qquad (1)$$

This photochemical H_2 elimination (Eq. 1) can be readily reversed by thermal H_2 addition with an energy release of approximately 15–20 kcal/mol.

$$\left[IrCl(PPh_3)_3\right] + H_2 \xrightarrow{\Delta} \left[IrClH_2(PPh_3)_3\right] + 15\text{–}20\,\text{kcal/mol}. \qquad (2)$$

Thus, the $[IrClH_2(PPh_3)_3]$-$[IrCl(PPh_3)_3]$ system offers a remarkable engine for hydrogen and energy storage.

The main purpose of the present study is to theoretically clarify the electronic process of the photochemical H_2 elimination of $[IrClH_2(PH_3)_3]$. We examine the electronic structures of several lower singlet excited states of the complex and the possibilities of both thermal and photochemical reactions.

2 Computational method

$[IrClH_2(PH_3)_3]$ is used as a model compound in the present study. The electronic structure of the singlet ground state of the system was calculated by the ab initio restricted Hartree-Fock (RHF) method for the geometry optimization and the second-order Møller-Plesset perturbation (MP2) method for the energy calculation, and those of the singlet excited states were calculated by the single excitation configuration interaction (SE-CI) method. The geometries for the energy minima and the transition state were determined by the energy-gradient method with the assumption of the C_s symmetry. The calculations were performed using the Gaussian 94 program [18]. The symmetry adapted cluster (SAC) [19] SAC-

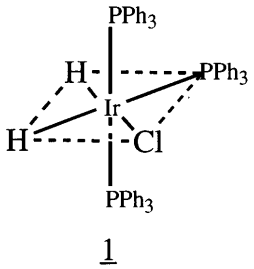

1

Fig. 1. The configuration of $[IrClH_2(PPh_3)_3]$

configuration interaction (SAC–CI) [20, 21] calculations were carried out using SAC85 [22] and its modified version [23].

The Gaussian bases for Cl and P used were the (3*s*3*p*)/[2*s*2*p*] sets replacing the Ne cores by the respective effective core potentials (ECPs) [24, 25]. For the Ir atom, the ECP of the Xe plus $4f^{14}$ core and the (3*s*3*p*3*d*)/[3*s*2*p*2*d*] set of the valence electrons were adopted [26]. The (4*s*)/[2*s*] set of Huzinaga-Dunning was used for hydrogen [27].

In the SAC/SAC–CI calculations of $[IrClH_2(PH_3)_3]$, all SCF molecular orbitals (MOs), 21 occupied and 54 unoccupied MOs, were included in the active space. All of the single excitations and selected double excitations within this active space constituted linked operators, and their products unlinked operators. The perturbation selection procedure [28, 29] was performed for the linked double operators with an energy threshold of 5×10^{-6} a.u. for the ground state and 5×10^{-7} a.u. for the excited states. The dimensions after the configuration selection are 15223 (324693: before selection) for the ground state and 30237 (324693) and 30735 (319986) for the excited states with A′ and A″ symmetry, respectively.

3 Thermal processes

The thermal reductive elimination of $[IrClH_2(PH_3)_3]$ and the thermal oxidative addition of H_2 to $[IrCl(PH_3)_3]$ are examined in this section. The geometry optimization and the single-point energy calculation were performed by the Hartree-Fock (HF) and MP2 methods, respectively. The geometry of the phosphine ligand was fixed throughout our calculations, namely, the P-H distance and the Ir-P-H angle were fixed at 1.42 Å and 122.75°, respectively.

We first performed the geometry optimization of the reactant, maintaining C_s symmetry. The calculated geometry parameters are shown in Fig. 2. The optimized geometry for $[IrClH_2(PH_3)_3]$ is calculated to be a six-coordinate octahedral conformation.

We next investigated the ground-state decomposition reaction of the reactant into $[IrCl(PH_3)_3] + H_2$. Fig. 3 shows the potential energy curves (PECs) for the decomposition of the reactant. The distance *R* between Ir and the centre of the H—H bond was adopted as the reaction coordinate. Other parameters were optimized at each point except for the PH_3 ligand. The optimized geometries in the decomposition process into $[IrCl(PH_3)_3]$ and H_2 are shown in Fig. 4. The product, $[IrCl(PH_3)_3]$, becomes four-coordinate square-planar at the separation of 5 Å.

The heat of the decomposition reaction is 15.3 and 21.1 kcal/mol by the HF and MP2 methods, respectively. These values are in a reasonable agreement with the experimental heat of the reaction, 15∼20 kcal/mol

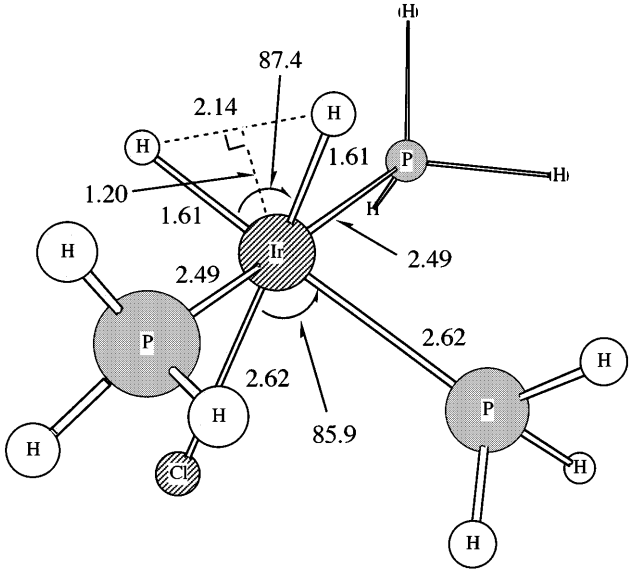

Fig. 2. Optimized geometry for $[IrClH_2(PH_3)_3]$ by the Hartree-Fock (HF) method

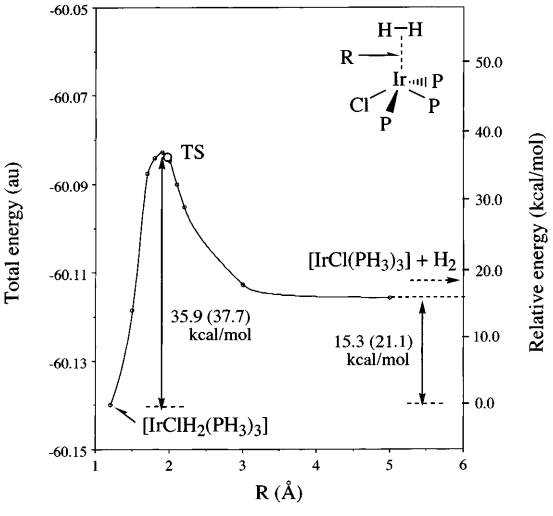

Fig. 3. Potential energy curve for H_2 elimination of $[IrClH_2(PH_3)_3]$ in the ground state by the HF method. The values in parentheses are obtained by single-point energy calculation using the second-order Møller-Plesset perturbation (MP2) method

[17]. The dissociation and the association barriers are calculated as 35.9 and 20.6 kcal/mol, respectively, by the HF method, and 37.7 and 16.6 kcal/mol, respectively, by the MP2 method. While the electron correlations are not small, the comparative energies such as the reaction heat or the energy barriers shifted less than 6 kcal/mol.

Since the Cl-Ir-P angle changes considerably near R = 1.9 Å, where the TS of the activation barrier exists as shown in Fig. 3, the geometrical change of the iridium complex from octahedral to square-planar causes the activation barrier of the process. The highest occupied molecular orbital (HOMO) of the system at R = 1.9 Å has a bonding character that is between the dπ atomic orbital (AO) of Ir and the sσ* MO of H_2. This interac-

tion corresponds to the typical π-back donation interaction in the Dewar-Chatt-Duncanson (D-C-D) model [30]. The HOMO involves the antibonding character between the dπ AO of Ir and the p AO of Cl and P. An elongation of the distance between Ir and H_2 results in a reduction of the Ir dπ–H_2 sσ* bonding interaction as well as an increase in the population of the Ir dπ-ligand antibonding orbital. This is the cause of the barrier. The antibonding interaction diminishes when the Ir complex is transformed into square-planar geometry.

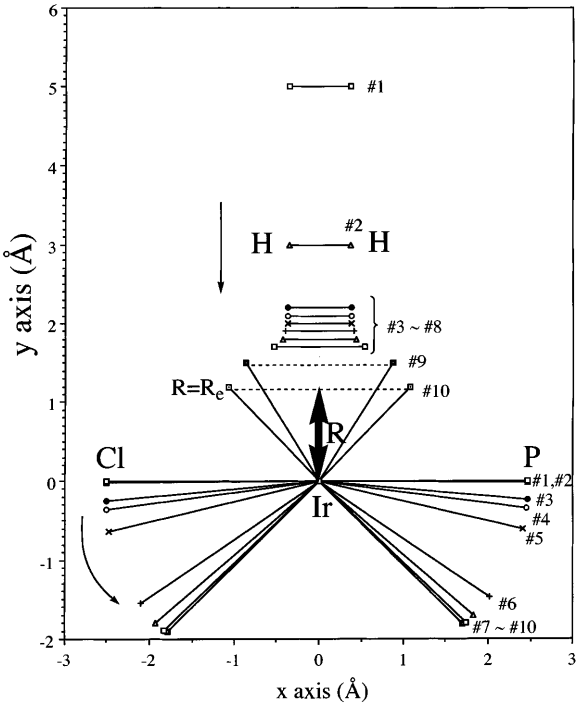

Fig. 4. Optimized geometries for H_2 addition and elimination processes in the ground state

In contrast, the π-back donation from Ir dπ AO to H_2 sσ* MO contributes to a decrease in the reaction barrier in the oxidative addition of H_2 with $[IrCl(PH_3)_3]$, which is the reverse reaction of reductive elimination.

These results show that the reductive elimination of H_2 from $[IrClH_2(PH_3)_3]$ does not proceed thermally, while the oxidative addition of H_2 to $[IrCl(PH_3)_3]$ would occur. This result and the calculated heats of oxidative addition agree with the experimental observations.

4 Photochemical processes

In this section, we study the photochemical reductive elimination of H_2 from $[IrClH_2(PH_3)_3]$. We first calculate the singlet vertical excitation energies of $[IrClH_2(PH_3)_3]$ at its equilibrium geometry by the HF/SE–CI and SAC/SAC–CI methods. Table 1 shows the excitation energy, the main configuration and the oscillator strength for the singlet excited states below 5.46 eV. Since the energy differences between the HF/SE–CI and SAC/SAC–CI methods are not so large for this molecule, the geometry optimization using the HF/SE–CI methods may be justified.

The experimental first shoulder peaks at about 3.8 eV and is assigned to $1^1A''$ (3.70 eV) due to the SAC–CI energy and oscillator strength. The experimental second

Table 1. Singlet excited states of $[IrClH_2(PH_3)_3]$ at the reactant geometry calculated by the SE–CI and SAC–CI methods

State	SAC–CI					SE–CI	Expt.[c]
	Main Configuration[a]			Oscillator strength	Excitation energy in eV (nm)	Excitation energy in eV (nm)	Excitation energy in eV (nm)
	Configuration	Character[b]	Coefficient				
X^1A'	HF		0.997		0.00	0.00	0.00
$1^1A''$	$6a'' \rightarrow 15a'$	$\sigma_{Cl} \rightarrow \sigma_P^*$	0.556	7.66×10^{-3}	3.70 (335)	3.61 (343)	3.82 (325)
	$8a'' \rightarrow 15a'$	$\sigma_{Cl} \rightarrow \sigma_P^*$	0.529				
$2^1A'$	$13a' \rightarrow 15a'$	$\sigma_{Cl} \rightarrow \sigma_P^*$	0.554	7.83×10^{-4}	3.74 (332)	3.83 (324)	
	$10a' \rightarrow 15a'$	$\sigma_{Cl} \rightarrow \sigma_P^*$	0.401				
	$13a' \rightarrow 14a'$	$\sigma_{Cl} \rightarrow \sigma_P^*, \sigma_H^*$	0.314				
$2^1A''$	$7a'' \rightarrow 15a'$	$d \rightarrow \sigma_P^*$	0.622	1.20×10^{-2}	4.29 (289)	4.07 (305)	
	$7a'' \rightarrow 14a'$	$d \rightarrow \sigma_P^*, \sigma_H^*$	0.509				
	$7a'' \rightarrow 16a'$	$d \rightarrow \sigma_P^*, \sigma_H^*$	0.420				4.77 (260)
$3^1A'$	$13a' \rightarrow 14a'$	$\sigma_{Cl} \rightarrow \sigma_P^*, \sigma_H^*$	0.482	2.94×10^{-3}	4.73 (262)	5.02 (247)	
	$13a' \rightarrow 15a'$	$\sigma_{Cl} \rightarrow \sigma_P^*$	0.444				
	$10a' \rightarrow 14a'$	$\sigma_{Cl} \rightarrow \sigma_P^*, \sigma_H^*$	0.399				
$3^1A''$	$8a'' \rightarrow 14a'$	$\sigma_{Cl} \rightarrow \sigma_P^*, \sigma_H^*$	0.594	1.90×10^{-2}	5.34 (232)	5.98 (207)	
	$8a'' \rightarrow 15a'$	$\sigma_{Cl} \rightarrow \sigma_P^*$	0.405				
	$6a'' \rightarrow 14a'$	$\sigma_{Cl} \rightarrow \sigma_P^*, \sigma_H^*$	0.360				
$4^1A'$	$12a' \rightarrow 15a'$	$\sigma_{Cl} \rightarrow \sigma_P^*$	0.721	1.63×10^{-1}	5.46 (227)	6.35 (195)	
	$12a' \rightarrow 14a'$	$\sigma_{Cl} \rightarrow \sigma_P^*, \sigma_H^*$	0.491				
	$12a' \rightarrow 16a'$	$\sigma_{Cl} \rightarrow \sigma_P^*, \sigma_H^*$	0.349				

[a] Configurations whose CI coefficients (absolute values) are more than 0.3 are shown
[b] σ_{Cl} and d indicate the Ir–Cl σ bonding orbital and the Ir d orbital, respectively. σ_P^* and σ_H^* indicate the Ir–P and Ir–H σ antibonding orbitals, respectively
[c] These experimental peaks are the shoulder of the large peak in the higher energy range

peak, which is reported to be a shoulder of the large peak in the higher energy range [17], may be assigned to either $2^1A''$ (4.29 eV) or $3^1A'$ (4.73 eV), the first assignment based on the larger oscillator strength and the second based on the excitation energy. Note that the experimental peak positions of these absorptions are rather hard to determine from their broad shoulder shapes. A large peak in the higher range is assigned to the $4^1A'$ state (5.46 eV). The $2^1A'$, $2^1A''$ and $3^1A'$ have a excitation nature from the metal dπ AOs to the metal-H_2 antibonding orbital. Consequently, the bonding between $[IrCl(PH_3)_3]$ and H_2 should be weakened in these excited states.

Figure 5 shows the PECs for reductive elimination in the singlet excited states. These PECs were calculated by the HF/SE–CI method using the geometries optimized for the ground state as shown in Fig. 4. Since the lowest A′ state is repulsive, the elimination reaction may proceed through this excited state.

Figure 6 shows the PECs for the H_2 elimination in the lowest excited singlet A′ state, where the geometries used were optimized for this lowest excited $^1A'$ state in the SE–CI approximation. There are several crossings and avoided crossings in the range of R = 1.2–2.0 Å. In particular, the crossing at R = 1.2–1.4 Å between the $1^1A''$ and $2^1A'$ states is very important. The SAC–CI results suggest that the photochemical reductive H_2 elimination starts from the vertical excitation to the $1^1A''$ state. Figure 6 indicates that the photochemical reaction proceeds via this $2^1A'$ state through the above crossing and would be relaxed to the ground state at R = 1.8 Å through the diabatic process. Notably, no photoluminescence is observed experimentally that supports the diabatic pathway.

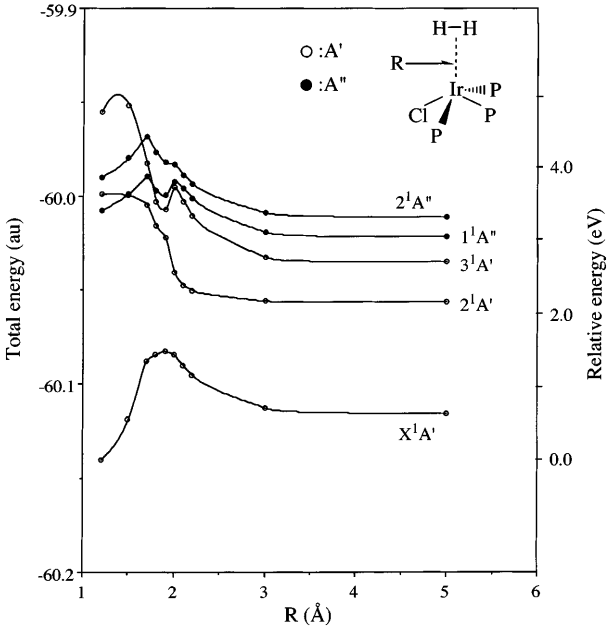

Fig. 5. Potential energy curves (PECs) for H_2 elimination in the singlet excited states, the geometries of which are optimized in the ground state

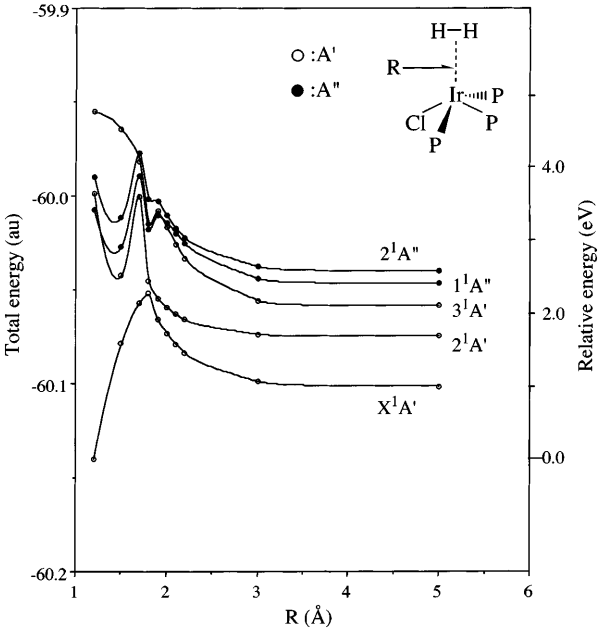

Fig. 6. PECs for H_2 elimination calculated with the optimized geometries in the lowest 1A′ excited state

5 Conclusion

We examined the mechanisms and pathways of the photochemical reductive elimination of H_2 from $[IrClH_2(PH_3)_3]$ and the thermal H_2 addition reaction to $[IrCl(PH_3)_3]$ by the ab initio MO theory using the HF, MP2, SE–CI and SAC/SAC–CI methods.

The energy barrier for the thermal H_2 elimination was calculated to be 35.9 and 37.7 kcal/mol by the HF and MP2 methods, respectively. This barrier is due to a decrease in the Ir (dπ)–H_2 (sσ*) bonding interaction as well as an increase in the Ir – ligands antibonding interactions. Therefore, H_2 elimination cannot proceed thermally.

On the other hand, since the π-back donation from Ir dπ AO to H_2 sσ* MO lowers the reaction barrier for thermal H_2 addition, as calculated to be 20.6 and 16.6 kcal/mol by the HF and MP2 methods, respectively, the H_2 addition reaction to $[IrCl(PH_3)_3]$ may proceed thermally. The heat of reaction obtained here shows fairly good agreement with experimental findings.

The lower excited states of $[IrClH_2(PH_3)_3]$ shown in Table 1 have the nature of the excitation from Ir to Ir-H_2 antibonding orbital, so that these excited states would facilitate the H_2 elimination reaction. In particular, the $1^1A''$ state is transferred to the $2^1A'$ state through the avoided crossing and the $2^1A'$ state would be relaxed to the ground state through the diabatic process.

Acknowledgements. This study was supported in part by a Grant-in-Aid for Scientific Research from the Ministry of Education, Science and Culture and partially by the New Energy and Industrial Technology Development Organization (NEDO).

References

1. Geoffroy GL (1980) Prog Inorg Chem 27: 123
2. Vaska L (1968) Acc Chem Res 1: 335
3. Vaska L, Diluzio JW (1961) J Am Chem Soc 83: 2784
4. Vaska L, Diluzio JW (1962) J Am Chem Soc 84: 679
5. Vaska L (1963) Science 140: 809
6. Vaska L, Bath SS (1966) J Am Chem Soc 88: 1333
7. Vaska L, Rhodes RE (1965) J Am Chem Soc 87: 4970
8. Vaska L (1966) Science 152: 769
9. Vaska L, Catone DL (1966) J Am Chem Soc 88: 5324
10. Vaska L, Chen LS, Miller WV (1971) J Am Chem Soc 93: 6671
11. McGinnety JA, Doedens RJ, Ibers JA (1967) Inorg Chem 6: 2243
12. Vaska L (1966) Proc Int Conf Coord Chem 9: 332
13. Doronzo S, Bianco VD (1972) Inorg Chem 11: 466
14. Vaska L (1966) J Am Chem Soc 88: 5325
15. Vaska L (1961) J Am Chem Soc 83: 756
16. Bennett MA, Milner DL (1969) J Am Chem Soc 91: 6983
17. Geoffroy GL, Pierantozzi R (1976) J Am Chem Soc 98: 8054
18. Frish MJ, Trucks GW, Schlegel HB, Gill PMW, Johnson BG, Robb MA, Cheeseman JR, Keith TA, Petersson GA, Montgomery JA, Raghavachari K, Al-Laham MA, Zakrzewski VG, Ortiz JV, Foresman JB, Cioslowski J, Stefanov BB, Nanayakkara A, Challacombe M, Peng CY, Ayara PY, Chen W, Wong MW, Andres JL, Replogle ES, Gomperts R, Martin RL, Fox DJ, Binkley JS, Defrees DJ, Baker J, Stewart JP, Head-Gordon M, Gonzalez C, Pople JA (1995) Gaussian Inc., Pittsburgh Pa. Gaussian 94 (Revision A.1)
19. Nakatsuji H, Hirao K (1978) Chem Phys 68: 2035
20. Nakatsuji H (1978) Chem Phys Lett 59: 362
21. Nakatsuji H (1979) Chem Phys Lett 67: 329, 334
22. (a) Nakatsuji H (1985) Program system for SAC and SAC–CI calculations, Program Library No 146 (Y4/SAC), Data Processing Center of Kyoto University; (b) Nakatsuji H (1981) Program Library SAC85, No 1396, Computer Center of the Institute for Molecular Science, Okazaki
23. Nakatsuji H, Hada M, Ehara M, Hasegawa J, Nakajima T, Nakai H, Kitao O, Toyota K (1996) SAC/SAC–CI Program System (SAC–CI 96) for calculating ground, excited, ionized, and electron-attached states and singlet, doublet, triplet, quartet, quintet, sextet, and septet spin states, (1996)
24. Hay PJ, Wadt WR (1985) J Chem Phys 82: 270
25. Hay PJ, Wadt WR (1985) J Chem Phys 82: 284
26. Hay PJ, Wadt WR (1985) J Chem Phys 82: 299
27. (a) Huzinaga S (1965) J Chem Phys 42: 1293; (b) Dunning TH Jr (1970) J Chem Phys 53: 2823
28. Nakatsuji H (1983) Chem Phys 75: 425
29. Nakatsuji H, Hasegawa J, Hada M (1996) J Chem Phys 104: 2321
30. (a) Dewar MJS, (1951) Bull Soc Chim Fr 18:C79; (b) Chatt J, Duncanson LAJ (1953) J Chem Soc 2339